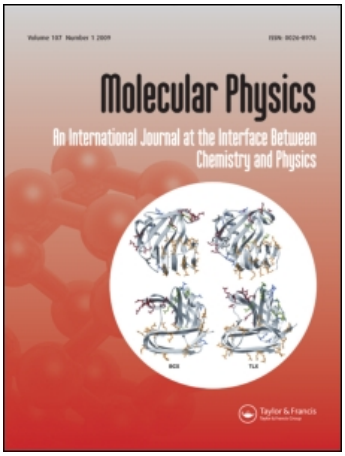

Molecular Physics
Publication details, including instructions for authors and subscription information:
http://www.informaworld.com/smpp/title~content=t713395160

Vibrational cooling of cold molecules with optimised shaped pulses

D. Sofikitis[a]; A. Fioretti[a]; S. Weber[b]; R. Horchani[a]; M. Pichler[ac]; X. Li[a]; M. Allegrini[ad]; B. Chatel[b]; D. Comparat[a]; P. Pillet[a]
[a] Laboratoire Aimé Cotton, CNRS, Université Paris-Sud, 91405 Orsay, France [b] Laboratoire Collisions, Agrégats, Réactivité (UMR 5589, CNRS-Université Paul Sabatier Toulouse 3), Toulouse, France [c] Department of Physics, Goucher College, Baltimore, MD, 21204, USA [d] CNISM, Dipartimento di Fisica, Università di Pisa, 56127 PISA, Italy

Online publication date: 26 April 2010

To cite this Article Sofikitis, D. , Fioretti, A. , Weber, S. , Horchani, R. , Pichler, M. , Li, X. , Allegrini, M. , Chatel, B. , Comparat, D. and Pillet, P.(2010) 'Vibrational cooling of cold molecules with optimised shaped pulses', Molecular Physics, 108: 6, 795 — 810
To link to this Article: DOI: 10.1080/00268971003689899
URL: http://dx.doi.org/10.1080/00268971003689899

Molecular Physics
Vol. 108, No. 6, 20 March 2010, 795–810

Taylor & Francis
Taylor & Francis Group

INVITED ARTICLE

Vibrational cooling of cold molecules with optimised shaped pulses

D. Sofikitis[a], A. Fioretti[a]*, S. Weber[b], R. Horchani[a], M. Pichler[ac], X. Li[a], M. Allegrini[ad], B. Chatel[b], D. Comparat[a] and P. Pillet[a]

[a]*Laboratoire Aimé Cotton, CNRS, Université Paris-Sud, Bât. 505, 91405 Orsay, France;* [b]*Laboratoire Collisions, Agrégats, Réactivité (UMR 5589, CNRS – Université Paul Sabatier Toulouse 3), IRSAMC, Toulouse, France;* [c]*Department of Physics, Goucher College, Baltimore, MD, 21204, USA;* [d]*CNISM, Dipartimento di Fisica, Università di Pisa, Largo Pontecorvo 3, 56127 PISA, Italy*

(*Received 10 November 2009; final version received 5 February 2010*)

A review of our recent experiments on broadband vibrational cooling of cold cesium molecules and of the related theory is presented. Our method is based on repetitive optical pumping cycles driven by laser light which is broad enough to excite all populated vibrational levels. Originally, the accumulation of molecular population in a particular, pre-selected vibrational level was achieved by removing from the broadband light all frequencies that could excite that vibrational level and thus making it a 'dark state' of the system. Here, we focus onto an additional, more sophisticated shaping method, which consists of selecting only specific frequency components that excite molecules into vibrational levels that favourably decay into the pre-selected level. The population transfer to any desired state can thus be optimised, i.e. the total population transfer to the desired vibrational level is maximised while the number of absorption–emission cycles required for the vibrational cooling is minimised. Finally, we apply this optimised technique to some more complex and still experimentally open cases: the pumping into the $a^3\Sigma_u^+$ ground state for the case of Cs_2 homonuclear molecules, the rotational pumping into a pre-selected ro-vibrational level and the NaCs as an example for heteronuclear molecules.

Keywords: cold molecules cooling; cold molecules; optical pumping; vibrational cooling; pulse shaping

1. Introduction

The manipulation of atomic or molecular quantum dynamics and the availability of robust and selective methods of performing population transfer in quantum systems is essential for a variety of fields, such as precision spectroscopy, quantum computing, control of molecular dynamics and chemical reactions [1–3].

In particular, the activities developed in the domain of cold molecules through precise control of both internal and external degrees of freedom of a molecule are expected to lead significant advances in collision dynamics of chemical reactions, molecular spectroscopy, molecular clocks, fundamental test in physics, controlled photo-chemistry studies, and quantum computation with polar molecules [4–8].

However, control of the internal molecular states is not straightforward. Due to their complex internal structure, the standard laser cooling techniques as developed for atoms [9] do not work for molecules [10] and other pathways are required. Methods, such as Stark deceleration or sympathetic cooling, start from pre-formed molecules. Usually they produce molecules in the lowest vibrational level, but with translational temperatures not lower than a few millikelvins [11]. Cold molecules in the micro- or nanokelvin temperature range can only be achieved starting from association of ultracold atoms either via magneto-association (Feshbach resonances) [6,12,13] or through photoassociation [14]. Both techniques produce translationally cold ($T \sim 100\,\mathrm{nK}$ for magneto-association and $T \sim 100\,\mu\mathrm{K}$ for photoassociation, respectively) molecular gases as cold as the atoms they are formed from, but they require additional efforts to cool the vibrational and rotational degrees of freedom. The main difference between these two association techniques is the nature of the mechanisms involved. Magneto-association via Feshbach resonances is a coherent process that can produce ultracold molecules in a single quantum ro-vibrational state. Photoassociation is an incoherent process involving a spontaneous emission step that produces ultracold molecules in a bunch of quantum ro-vibrational states. Very recently coherent optical schemes have been very successful in selectively producing ultracold, dense samples of deeply bound molecules in the vibrational ground state [15–18]. Even if very powerful for molecules

*Corresponding author. Email: andrea.fioretti@lac.u-psud.fr

ISSN 0026–8976 print/ISSN 1362–3028 online

DOI: 10.1080/00268971003689899
http://www.informaworld.com

produced by the Feshbach technique, such a coherent STIRAP (Stimulated Raman Adiabatic Passage) process can only transfer population from one state to another one, and therefore cannot transfer population from an ensemble of vibrational levels into a single state as needed for molecules prepared via photoassociation. In these cases, other solutions are required, for instance various schemes can favour the formation of photoassociated cold molecules in their lowest vibrational level as experimentally demonstrated [19–21], or theoretically proposed [6,22–28]. However, in analogy to atoms, optical pumping for molecules would really be the best way to transfer all the population from different ro-vibrational levels into a single one and therefore to realise ro-vibrational laser cooling.

Using pulse shaping techniques, we have previously partially achieved this goal by demonstrating optical pumping for the vibrational degree of freedom of a molecule [29]. It was indeed natural to use the fact that shaped femtosecond laser pulses can manipulate the internal degree of freedom of molecules [30], as proposed theoretically [31–34] and experimentally investigated with cold molecules [35,36]. These pulse shaping techniques, which permit one to control the phase as well as the amplitude of each spectral component of the laser pulse, have been reviewed in detail [37] and have led to important results in coherent control [30,38–40], compression of optical pulses [41] and optical communications [42].

Here we report on our recent experiments that have exploited two different shaping methods for vibrational cooling. The first is based on the creation of dark states, while the second is a more sophisticated method in which only transitions optimising population transfer into a pre-selected vibrational level are kept. The paper is organised as follows: we first describe our experimental apparatus in its main parts, namely the Magneto-Optical Trap (MOT) where the cold Cs_2 molecules are produced and the pulse shaping apparatus based on a Liquid Crystal Spatial Light Modulator (LC-SLM) is placed in the Fourier plane of a highly dispersive 4f line [43]. Then we present the selective vibrational cooling of the molecules into a given vibrational level on demand. Examples are reported for the vibrational levels $v=0$ and $v=1$. Population transfer to $v=1$ is demonstrated with both shaping methods and the results produced by each one are discussed. In the following paragraphs, we study several difficult cases, where the simple, frequency-removing shaping is not expected to lead to considerable results, while the optimised shaping technique does. These cases include: cooling cesium dimers in the ground $a^3\Sigma_u^+$ triplet state, balancing the heating effect on the molecular vibration due to the laser addressing the rotation and cooling the vibration of the NaCs molecule chosen as a case to illustrate the extension to heteronuclear dimers. Finally, we draw the conclusions and discuss the perspectives for direct laser cooling of molecules, based on this optimised shaping method.

2. Vibrational cooling of singlet Cs_2 molecules with shaped femtosecond pulses

2.1. *Basics of the optimised molecular population trasfer*

Some of us have recently published an experimental realisation of the vibrational cooling in the ground singlet state of Cs_2 based on optical pumping using several identical weak femtosecond laser pulses [29]. Cs_2 molecules initially formed via photoassociation (PA) of cold cesium atoms in several vibrational levels, v, of the electronic ground state were redistributed in the ground state via a few electronic excitation–spontaneous emission cycles by applying a femtosecond broadband laser. The laser pulses were shaped to remove the excitation frequency band from the $v=0$ level, thus preventing *excitation from* and leading to an efficient *accumulation into* this lowest vibrational level of the singlet electronic ground state. Subsequently, using the flexibility of femtosecond pulse shaping techniques [37], this population pumping method has been extended in order to accumulate molecules into a single selected vibrational level other than the $v=0$ one [44].

The main idea in the vibrational optical pumping as performed in [29], is to use a laser with a broadband spectrum tuned to a bunch of electronic transitions between different vibrational levels of the molecule, which we label v_X and v_B, belonging respectively to the singlet-ground-state $X^1\Sigma_g$, hereafter simply referred to as X, and to an electronically excited state, for instance the $B^1\Pi_u$ state of the Cs_2 system, hereafter referred to simply as B. The goal is to start from a given vibrational distribution of v_X values, as obtained after the PA, and to transfer it into a single targeted vibrational level. The absorption–spontaneous emission cycles lead, through optical pumping, to a redistribution of the vibrational population into the ground state. The broadband character of the laser allows repetition of the pumping process from multiple vibrational v_X levels. By removing the laser frequencies corresponding to the excitation of a selected v_X level, we prevent molecules to be pumped out of it, thus making this level a dark state. As time progresses, the series of absorption–spontaneous emission cycles leads

to an accumulation of the molecules into the selected v_X level.

The core of the experiment is a cesium vapour-loaded MOT where nearly 10^8 atoms are continuously laser cooled and trapped at a temperature of $T \sim 100\,\mu K$ and at a density of nearly $n \sim 10^{11}\,cm^{-3}$. The initial sample of cold molecules is obtained via photoassociation, a process where two cold colliding atoms resonantly absorb a photon to create a molecule in an excited electronic state that can decay into stable deeply bound vibrational levels of the singlet molecular ground X state. These molecules are available for further studies for about 10 ms before leaving ballistically the MOT region. Details on the experimental setup and methods can be found in [29,44,45] and in references therein. The laser transitions used are summarised in Figure 1 together with the relevant potential curves of the cesium dimer. PA is achieved using a cw Titanium : Sapphire laser (intensity $300\,W\,cm^{-2}$) pumped by an Ar^+ laser. This laser is red-detuned by roughly $2\,cm^{-1}$ with respect to the $6s \rightarrow 6p_{3/2}$ atomic transition, resonant with an excited molecular level. After spontaneous decay, the distribution of the molecules spans the $v = 1$–10 levels of the X ground state. Details of this PA mechanism are in [45].

Molecules are then ionised by Resonantly Enhanced Multiphoton Ionisation (REMPI) through the excited $C^1\Pi_u$ molecular intermediate state, hereafter referred to as C. The REMPI detection uses a pulsed dye laser (wavenumber $\sim$16,000 cm^{-1}, spectral bandwidth $0.3\,cm^{-1}$) pumped by the second harmonic

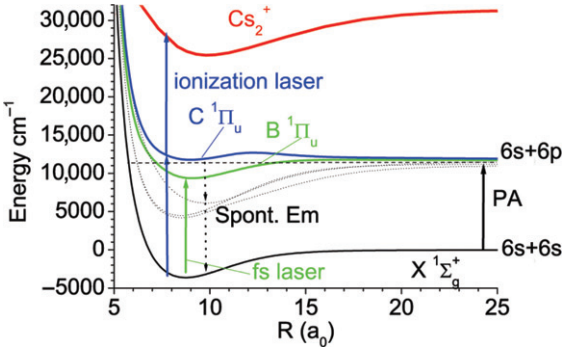

Figure 1. The cesium dimer potential curves relevant for the experiment. Cold atoms are excited at long range by the PA (black arrow) laser into a molecular excited level that subsequently decay through two spontaneous emissions into a stable molecule in a vibrational level of the ground X state. The shaped femtosecond laser (green arrow) pumps the produced molecules, via the intermediate excited B state (green dashed line), into a single selected vibrational level of the X state. Molecules are finally selectively ionised by two-step REMPI ionisation via the intermediate excited C state (solid blue).

of a pulsed Nd : YAG laser (repetition rate 10 Hz, duration 7 ns). The formed Cs_2^+ ions are detected using a pair of microchannel plates through a time-of-flight mass spectrometer. By scanning the REMPI laser wavelength, transitions from vibrational ground $v_X = 1$–10 levels to various levels v_C of the C state are monitored and assigned according to [46]. Any redistribution of population among the vibrational levels of the ground state introduced by some additional laser light results in a clear change in the relative intensities of the lines present in the spectrum. The molecular distribution among different levels can thus be monitored [29,44]. Conversely, the low resolution of these REMPI spectra do not provide, at present, the capability of analysing the rotational distribution of the molecular sample.

A series of shaped femtosecond laser pulses are used to achieve vibrational cooling. It is provided by a Kerr-Lens-Mode-locking Titanium : Sapphire oscillator with a repetition rate of 80 MHz (12.5 ns between subsequent pulse). The central wavelength is tuned at 773 nm. Its spectral Full Width at Half Maximum (FWHM) is around 10 nm.

In order to control the optical pumping, the spectrum of this femtosecond laser is first dispersed with a folded, zero-dispersion 4f-line and then shaped by either a simple razor blade [29] or by a high resolution pulse shaper [44], both alternatively placed in the Fourier plane of the line. The pulse shaper is composed of a dual LC-SLM which allows phase and amplitude modulation [47]. The LC-SLM (Jenoptik, SLM-S640/12) possesses 640 pixels and has been described in [48] (stripes of $97\,\mu m \times 10$ mm separated by gaps of $3\,\mu m$).

The regions of liquid crystal between the patterned electrodes cannot be controlled and are referred to as gaps. The presence of these gap regions and a non-perfect polarisation of the laser beam limit the on–off (extinction) ratio of the LC-SLM to a measured value of $\sim$3% of the light intensity in the worst case. In the simulations of the experiment this 3% conservative value is taken as the reference.

The characteristics of the LC-SLM setup reported in Figure 2 provide an average resolution of 0.06 nm $pixel^{-1}$ and a shaping spectral width of 38 nm, which is large enough to transmit the spectral pedestal width of our laser source (FWHM of 10 nm). The setting time inherent to these liquid-crystal devices (20 ms) does not represent a limitation for this experiment because the LC-SLM configuration was not changed within a single spectrum. In the present experiment an average femtosecond laser power of only 3 mW is used and focused on the molecular cloud with a waist of nearly

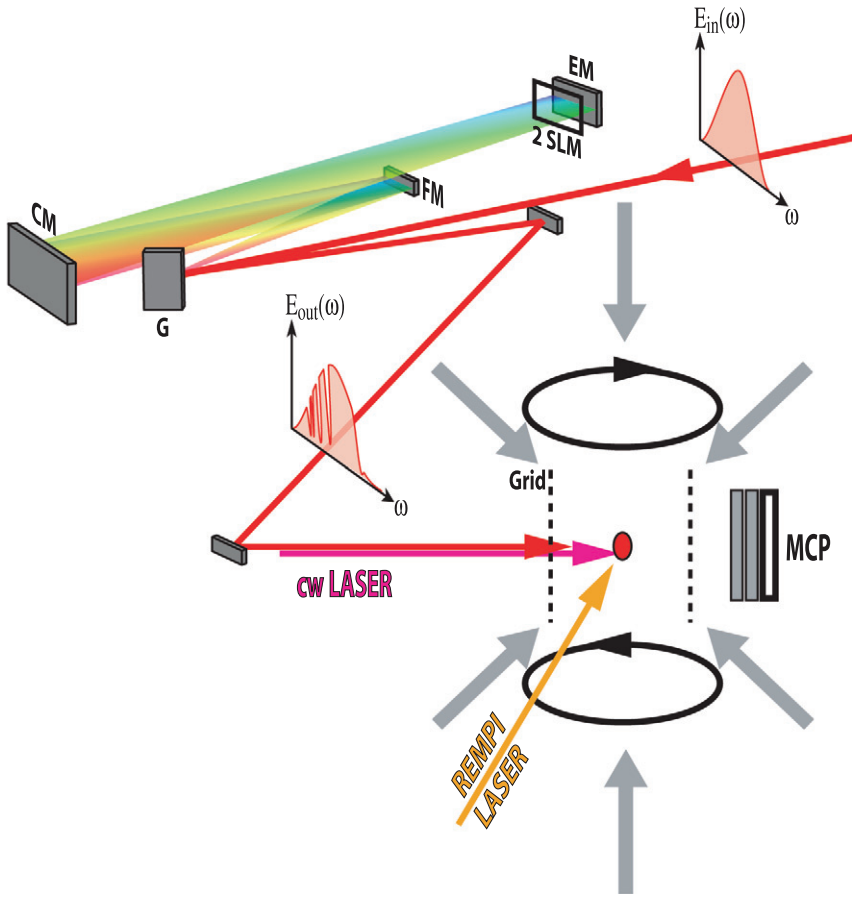

Figure 2. Experimental setup for the pulse shaper and the cold molecule production and detection. Upper part: folded, zero-dispersion 4f-line. The beam is dispersed by the grating G to spatially separate different frequency components. The cylindrical mirror CM then focuses each spectral component in the Fourier plane. FM is a plane folding mirror. Two LC-SLMs are at the Fourier plane. An end mirror EM is placed just after the LC-SLM so that the beam goes twice through the half of the line. The shaped light is then sent through the cold molecular cloud that is created by PA of cesium atoms, and laser cooled by a standard six-beam vapour-loaded MOT. The molecules are detected using a REMPI ionisation laser creating Cs_2^+ ions, which are accelerated by an electric field (created with the two grids surrounding the cloud) and monitored using a pair of micro-channel plates (MCP).

500 μm, corresponding to an intensity of 700 mW cm^{-2}. A similar value is used in the simulations.

2.2. *The $v_X = 0$, vibrational cooling case*

The first experimental realisation of the vibrational cooling was obtained by truncating the laser spectrum in the blue region by placing a simple razor blade [29] in the Fourier plane [49] of the 4f-line. For the cesium dimer, the frequencies that correspond to excitation of the ground vibrational level $v_X = 0$ to any vibrational level of the B potential lie higher than a 13,000 cm^{-1} threshold. Consequently, the shaped spectrum required to pump molecules *into* the $v_X = 0$ vibrational level is simply the usual laser spectrum truncated at this threshold. This result is easily recovered also by means of our LC-SLM setup. The experiment is presented in Figure 3(a), where the pulse used in experiment and simulation (left part), the result of the numerical simulation (middle), and finally the ionisation spectrum (right) are shown. The spectrum plotted with a black line in this graph, corresponds to a situation where the femtosecond radiation is blocked and thus no vibrational cooling is obtained. In this case, the ionisation spectrum is very rich and shows many peaks corresponding to different $v_X \rightarrow v_C$ transitions, as assigned in [29,45]. The ionisation spectrum plotted in Figure 3(a), obtained after the application of 10,000 cooling pulses, clearly shows that all transitions corresponding to ground levels other than $v_X = 0$

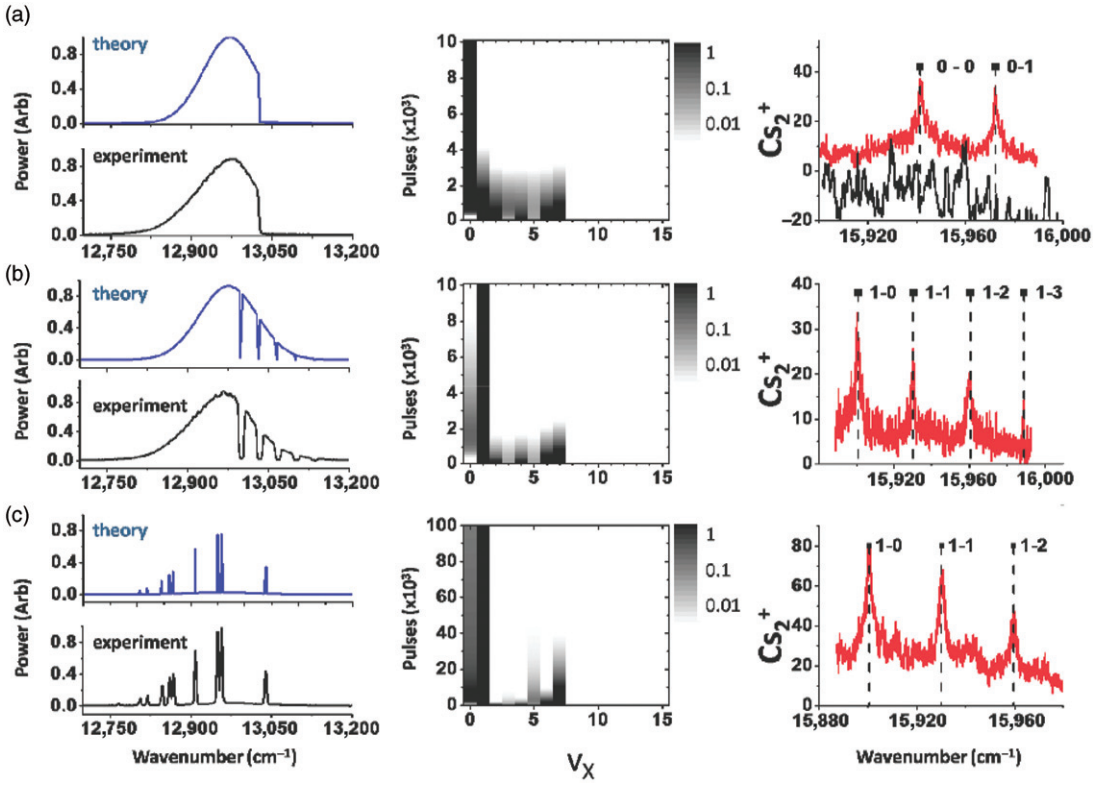

Figure 3. (a) In the left part, the simply shaped pulse, similar to the one used in [29]. The lower, black trace corresponds to the pulse actually used in the experiment, while the upper blue trace is a theoretical pulse used in the simulations. In the middle, a numerical simulation showing that 67% of the molecular population is accumulated in the $v_X = 0$ target state after application of 10,000 pulses. In the right part the ionisation spectra, with the black line corresponding to the situation where no shaped laser is present and the red line after the application of 10,000 pulses. The strong lines emerging in the second case, originate from a single v_X level, as shown by the labels. In part (b), the pulse (left), the simulation (middle) and the experimental results corresponding to molecular population transfer to the $v_X = 1$, which has now been chosen as the target state. In (c) the same goal is achieved with the alternative, optimised shaping technique.

disappeared, while those corresponding to the $v_X = 0$ level are strongly enhanced, and thus proves experimentally the success of the vibrational cooling process.

In order to predict the best possible laser spectrum to laser cool the molecular vibration, we have modelled the optical pumping in a very simple way. Using the known X, B potential curves and their rotational constants [50,51], we calculate the ro-vibrational energy levels as well as the Franck–Condon (FC) factors for the transitions. Because of the very low average laser intensity we are in a perturbative regime. Thus, we assume that the excitation probability is simply proportional to the laser spectral density at the transition frequencies, the FC factor, and the Hönl–London factor. If needed, rate equations could be determined, and solved exactly using for instance kinetic Monte Carlo modelling [52]. As less than one photon is absorbed during the excited state lifetime (~15 ns), we simply assume total population decay before sending, 12.5 ns later, another broadband light pulse. Initially, in each simulation, the molecules lie in the levels $v_X = 1$ to 10, with a distribution measured experimentally in [29]. Other processes, like three-photon direct ionisation by the femtosecond laser or pre-dissociation, are estimated to be not relevant for the experiment and are not taken into account by the simulation.

The overall efficiency of the vibrational cooling technique, i.e. the percentage of the molecular population finally transferred into the $v_X = 0$ 'target' vibrational level cannot be experimentally estimated at this point. This is mostly due to the fact that the initial number of molecules cannot be accurately known. However, an estimation of the efficiency can be provided by the numerical simulation shown in the middle part. There, a 67% of the total molecular population, which is initially distributed in the first 10 vibrational levels (in a known distribution,

experimentally obtained in [29]), is finally transferred to the target state.

2.3. *Population transfer to states with $v_X > 0$*

The idea of removing the frequencies that correspond to (all) possible excitations of a particular vibrational level, in order to form a dark state where molecular population can be accumulated by optical pumping, can be applied not only to the $v_X = 0$ level but to a number of selected levels. However, choosing a level different from the ground vibrational level as the target state for the molecular population transfer, imposes more complicated shaping. In the previous case where the ground $v_X = 0$ level was the 'target' state it was possible, by removing the part of the pulse lying above the 13,000 cm^{-1} threshold ($v_X = 0 \rightarrow v_B = 0$), to block all the frequencies that could excite the ground $v_X = 0$ level, and thus make it a 'dark state', without blocking other frequencies exciting other levels in the ground state. If we consider population transfer to the $v_X = 1$ level, we see that if we try to block all the frequencies above a similar threshold (corresponding to $v_X = 1 \rightarrow v_B = 0$), we will also block all frequencies that can excite the ground $v_X = 0$ vibrational level. Thus, instead of a unique dark state we have two, and the molecular population is going to be shared among them. A more refined frequency shaping method is needed.

This experimental complication has been initially overcome with the use of a setup employing the LC-SLM. In each case, the required spectrum is first calculated, relying on the known spectroscopy of the $X \rightarrow B$ transitions [46], and then implemented on the femtosecond laser by the LC-SLM. The example of pumping the molecular population in the $v_X = 1$ vibrational level, is shown in Figure 3(b). In the left part the theoretically computed and experimentally used pulses are shown. In the middle the results of the numerical simulation are shown. Note that the theoretical pulse used in the simulations takes into consideration the SLM's non-perfect extinction ratio (~3%). Finally, in the right part, we see the REMPI spectra obtained after the application of ~10,000 pulses as the ones shown in the left part. The efficiency of the molecular population transfer is estimated with the use of the numerical simulation to be ~53% in the $v_X = 1$ case. In principle, any vibrational level can be chosen as the target state. The obvious limitation lies upon the available laser bandwidth and upon the initial molecular distribution. The laser has to be strong enough in the vicinity of transitions between the initial states and the target one.

The efficiency of the population transfer process depends on various parameters: the FC factors, i.e. the relative position of the electronically excited potential curve with respect to the ground state one, the bandwidth of the femtosecond pulse used and the extinction ratio of the pulse shaper. However, it is possible to improve this efficiency, by choosing a different, more sophisticated shaping. This is demonstrated in Figure 3(c), and the aim is again to transfer as much of the molecular population as possible into the $v_X = 1$ vibrational level. In the left part, the (theoretical and experimental) pulses used in simulation and experiment are shown. The result of the numerical simulation is displayed in the middle, while in the right part we see the REMPI spectra obtained after application of 100,000 pulses similar to the ones presented in the left part. We notice that the increased number of laser pulses is necessary because the photon absorption probability during each pulse is reduced. The efficiency, i.e. the percentage of the total population which is finally transferred to the $v_X = 1$ 'target' level, is again estimated with the use of the numerical simulation. In this case, where the optimised shaping is used, a 67% of the total population is transferred to the target state, while this number is limited mostly due to the non-perfect (3%) extinction ratio of the SLM.

2.4. *Optimised vibrational cooling of the ground X singlet state of Cs_2 molecules: some details*

In order to understand the idea behind this new, more sophisticated pulse shaping, we consider the FC coefficients corresponding to the first 15 vibrational transitions. These coefficients can be plotted in a grey scale to form the so-called Condon parabola. In Figure 4, we display the parabola corresponding to the $X \rightarrow B$ electronic transition twice. In part (a), the Condon parabola is given along with a plot of the power per transition of a simply shaped pulse, similar to the one shown in the left part of Figure 3(b). The hatched area corresponds to those transitions which are addressed by the simply shaped pulse, down to the point where the laser power has reached 10% of its peak value. In part (b) the same Condon parabola is shown with a pulse power plot corresponding to an optimised shaped pulse as the one shown in the left part of Figure 3(c). With the arrows, we indicate several transitions which take place during the optical pumping process.

For example in Figure 4(a), we see that molecular population, initially in $v_X = 4$, can be excited to the $v_B = 1$ vibrational level. From there, spontaneous emission transfers population to several v_X vibrational

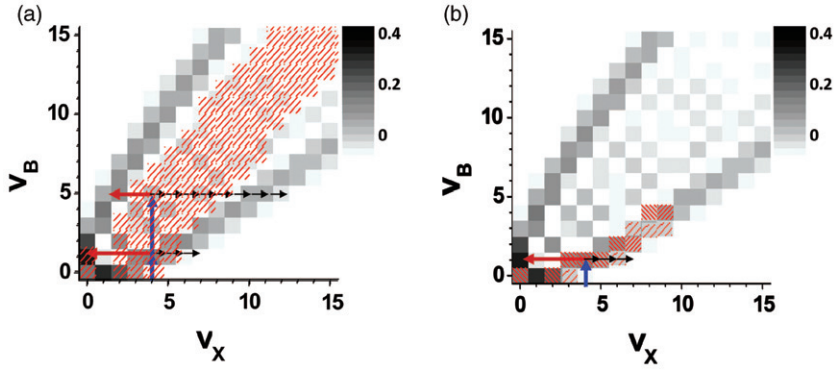

Figure 4. (a) Franck–Condon factors for the $X \rightarrow B$ transitions (grey levels), along with a plot of the laser power corresponding to each transition. The red-hatched area indicates the energy range covered by the shaped pulse shown on the left part of Figure 3(b). The frequency components for which the laser power is less than 10% of its maximum value are not shown. (b) The same FC factors for which fewer transitions are excited because of the optimised shaping shown in Figure 3(c).

levels, with a branching ratio proportional to the value of the corresponding FC coefficient. Thus, a part of the molecular population is transferred to the desired $v_X = 1$ level. Since the $v_X = 1$ is a dark state, all this population is no longer excited and exits the optical pumping process. However, for most of the population this is done in several absorption–spontaneous emission cycles. In this example, the largest part of the population is transferred to the $v_X = 0$ level, due to the relative magnitude of the corresponding FC coefficient, while population is also transferred to several higher vibrational levels as indicated by the arrows. As the process is repeated more and more, a large part of the population will be accumulated into the targeted $v_X = 1$ level. Nevertheless, a non-negligible part is also excited in high-lying vibrational states which lie outside the excitation spectra of the cooling pulse, and also exits the optical pumping process, contributing to the reduction of the population transfer efficiency. Finally, this simply shaped pulse can excite also molecules to high vibrational levels that are not 'connected' to the desired $v_X = 1$ level with high FC factor. In Figure 4(b), we show that with the use of an optimised shaped pulse most of these problems are overcome. For example, we can avoid excitation to high vibrational v_B levels that lead to loss of population. Additionally, the fact that only the lower branch of the Condon parabola is excited makes most of the spontaneous emission take place towards low vibrational levels. Thus, losses due to excitation to high v_B states are minimised, as indicated by the comparison between the results of the numerical simulations shown in the middle parts of Figure 3(b) and (c). We noticed, although the number of pulses (and thus the time) required to put the maximum fraction of molecules into the target level is larger for the optimised pulse than for the simple one, the expected number of absorption–spontaneous emission cycles is still smaller, due to the reduced excitation probability per pulse in the optimised case.

The efficiency of population transfer depends mainly on two effects: the limited bandwidth of the femtosecond laser and the non-zero extinction ratio of the LC-SLM. When molecules are pumped by excitation–spontaneous emission cycles, depending on the specific FC values, they can decay also into higher lying vibrational levels, where they become less and less resonant with the laser light, until they finally exit the cooling process and remain unaffected by the femtosecond laser. On the other side, the non-perfect extinction ratio, predominant for instance in the $v_X = 1$ case, depends on the residual 3% of laser light resonant with transitions from the target level, which has the deleterious effect of pumping molecules out of the dark level. Both these two reasons that reduce the population transfer efficiency can be taken into consideration, at least at a theoretical level. First, we can consider shaping the pulse with a perfect extinction ratio. Even though this possibility did not exist in our laboratory at the time of the experiment, it is well within the current technological capabilities, since the shaping can be performed with the use of a photo-mask, or with the use of mechanical shutters in the place of the liquid crystal inside the LC-SLM device.

In Figure 5 we present a simulation of population transfer to the ground $v_X = 0$ vibrational level in Cs_2 molecules. The pulse is shaped according to Figure 4(b), while the bandwidth (i.e. the FWHM) is raised to $165\,cm^{-1}$ and a perfect extinction ratio is considered. As we see in Figure 5(b), the effect of this optimised pulse is that practically all (~99.4%) the

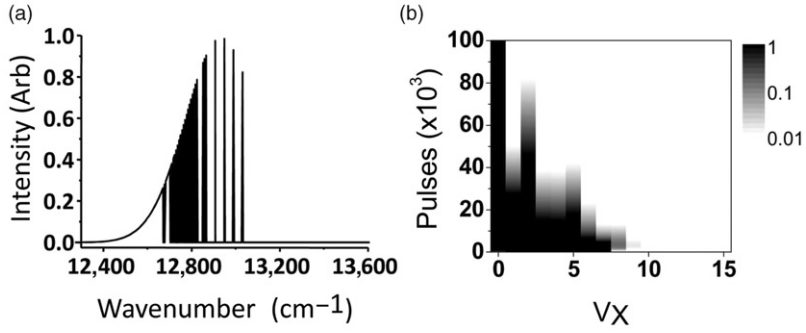

Figure 5. Simulation for the population transfer to $v_X = 0$, but with the use of a broader shaped pulse (but with the same total intensity) and with a perfect off-on extinction ratio. (a) The shaped pulse used for the simulation. The bandwidth is now three times larger than the one of the previous pulses ($165\,cm^{-1}$). (b) Results of the simulation of the vibrational cooling. The population of the $v_X = 0$ level after 10^5 pulses is 99.4%.

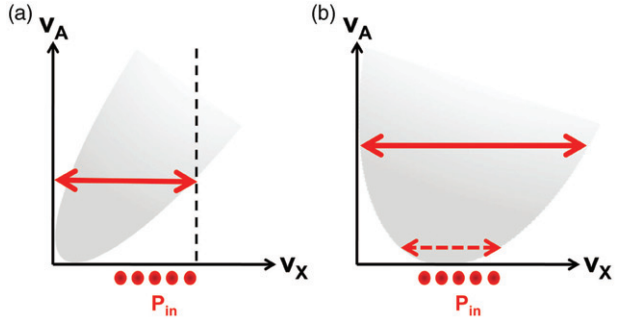

Figure 6. Bandwidth requirements for optical pumping of molecules. The initial vibrational population distribution P_{in} is indicated by the red dots. (a) A favourable situation where the intersection of the Condon parabola with the v_X axis is in the lower v_X levels. The required bandwidth for the achievement of optical pumping and vibrational cooling in such a situation is indicated by the arrow. (b) A less favourable situation, where the intersection of the Condon parabola with the v_X axis occurs in higher v_X states. If population transfer to the $v_X = 0$ is desired, the optical pumping process is such that the spread of the population in all states between the intersection of the Condon parabola with the v_A axis and the lower branch of the parabola, and the required bandwidth, which is noted by the arrow, is larger. The dotted arrow shows the bandwidth required to maintain an optical pumping process between the initially populated vibrational levels. A laser of that bandwidth can be shaped to achieve population transfer to a single level within the initially populated ones, but it cannot result in molecular population transfer to the ground vibrational level.

molecular population is transferred to the ground vibrational level.

2.5. *Requirements on laser bandwidth*

The requirements on the laser bandwidth depend strongly on the shape of the Condon parabola associated with the transition. For example, in Figure 6, we show two situations, a favourable and a less favourable one, in order to illustrate how Condon parabolas are linked to requirements for the laser bandwidth. In the favourable case (a), the Condon parabola is such that it intersects with the v_X axis in positions corresponding to the low v_X states. The molecular population is initially distributed in states that lie (in general) in higher v_X states. Simultaneous excitation of these molecules and preservation of an optical pumping process is possible if our pulse covers the area below the frequency indicated by the arrow. Indeed, if the laser bandwidth covers this area the absorption–spontaneous emission processes maintain the vibrational population v_X between 0 and the highest v_X initially populated. In part (b), we see a less favourable case of Condon parabola, where the intersection with the v_X axis is shifted to higher vibrational levels. The initial molecular population distribution is similar as before. If our goal is to transfer all molecular population to the $v_X = 0$ ground vibrational level (i.e. vibrational cooling), it is relatively easy to see that in order to excite molecular population in v_A levels that can relax to the lower v_X states, we need to access transitions in the central part of the Condon parabola. Spontaneous emission spreads the molecular population distribution as it transfers population to states with lower as well as with higher vibration. As a consequence, the bandwidth required to maintain an optical pumping process between all these levels is increased, as noted by the arrow.

It is interesting to see that if population transfer to the $v_X = 0$ ground vibrational level is not the goal, the optical pumping process can be considered between much fewer vibrational levels, and the required bandwidth, indicated by the dotted arrow, is much smaller. Such an optical pumping process can be useful for a

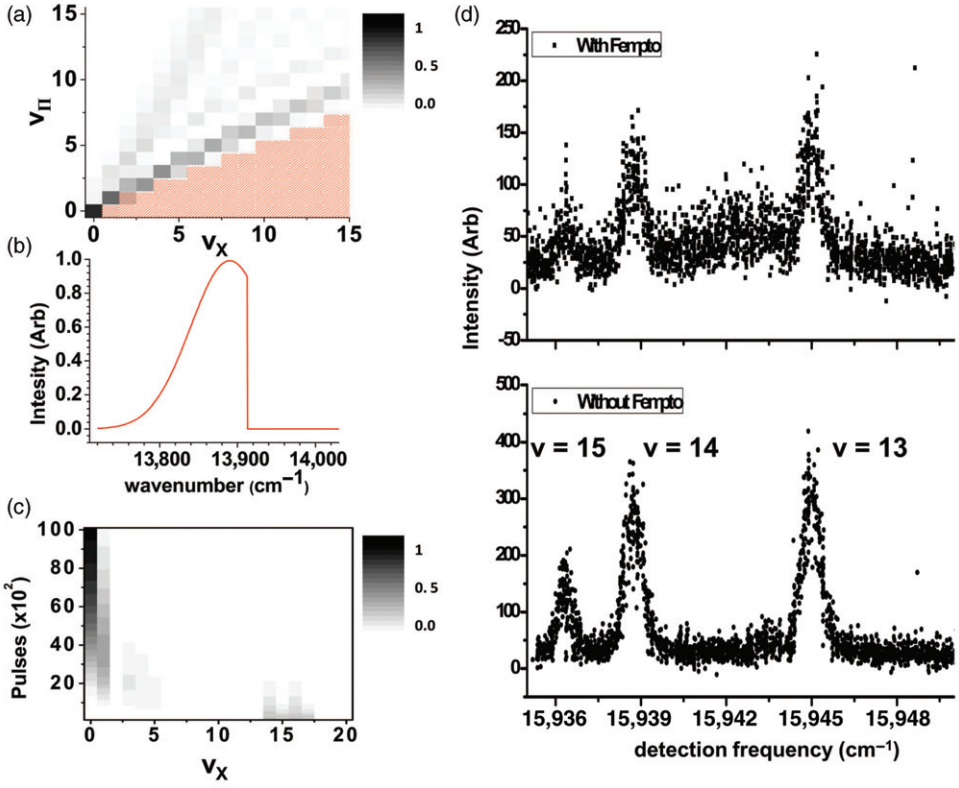

Figure 7. Simulation and experimental results for the vibrational cooling in the $a^3\Sigma_u^+$ triplet state via the $(2)^3\Pi_g$ state. In (a) a plot of the Condon parabola in grey scale is given, while in (red) hatches are marked the transitions excited by the shaped pulse shown in (b). In (c) a simulation of vibrational cooling in these conditions which leads to the accumulation of 91% of the molecules in the ground vibrational level. In the right part, results of the preliminary experimental study for the cooling in the triplet state. (d) Ionisation spectrum of the $a^3\Sigma_u^+$ molecules in the area of 15,950 cm^{-1}, where the assignment of the vibrational levels is done according to [53].

variety of purposes, as for example population transfer to a vibrational level different from $v_X = 0$, or to balance the heating effect of a rotational cooling process (see Section 4). Finally, from an experimental point of view we see that for the case of Cs_2 molecules, the bandwidth available by commercial femtosecond lasers (~10 nm) is sufficient due to the favourable shape of the Condon parabola associated with the X–B transition. In our simulations we are considering bandwidth similar or sometimes a few times larger than this. Increasing the bandwidth by a small factor (four or five) is enough for all the cases that we are going to examine in this article, which include less favourable Condon parabolas for the case of heteronuclear molecules. This is well within the present technological capabilities, since several broad-band sources, like the supercontinuum sources, can be considered for the optical pumping.

3. The case of $a^3\Sigma_u^+$ triplet state

One of the applications of the vibrational cooling technique considers the cooling of cesium dimers in their $a^3\Sigma_u^+$ triplet state. The motivation for cooling Cs_2 molecules in the ground triplet state is because photoassociation can provide triplet molecules in much larger numbers than singlet molecules [45]. The lifetime of the Cs_2 triplet state is on the order of some seconds. Therefore, they are considered stable enough for a variety of studies, while the number of problems that are easier to solve in the laboratory with the use of the huge triplet signal, is more than appealing.

Optical pumping of molecules that lie in the $a^3\Sigma_u^+$ triplet state was initially considered via the $(2)^3\Pi_g$ state, hereafter referred to as Π, due to the fact that the separation between the equilibrium distances between these states and the ground state is minimised. In the left part of Figure 7(a), the Condon parabola corresponding to the considered transition is displayed. The hatched area corresponds to those transitions excited by the shaped femtosecond pulse shown in Figure 7(b), for which the laser field has power larger than 0.001 of its maximum power. The resulting accumulation in the $v_X = 0$ level is shown in Figure 7(c).

However, our preliminary experiments to investigate the possibility of cooling the cesium dimers in their $a^3\Sigma_u^+$ triplet state, did not give the expected results. As for the singlet state molecules, the study of vibrational cooling is done by comparing the vibrationally resolved REMPI spectra obtained in the presence and in the absence of the cooling radiation. In the right part of Figure 7, we see a set of experimental results, corresponding to this study. The study is done at two different detection frequencies. Triplet molecules can be detected via a REMPI ionisation either in the region between 13,500 and 14,500 cm^{-1} for ionisation through the $(2)^3\Sigma_g$ and the $(2)^3\Pi_g$ electronic state, or in the region between 15,900 and 15,950 cm^{-1} for ionisation through the $(3)^3\Sigma_g$ one. We report the results obtained in the second region, where the spectroscopic lines are more separated and their position has been assigned [53]. In any case, the exact position of each spectroscopic line is of small significance. What is of importance here, is that in all these spectra, no structural difference between spectra acquired in the presence and in the absence of the femtosecond radiation is observed, but only the spectra acquired in the presence of the cooling field have somehow reduced signal. This means that the molecular population that was initially excited, did not return to the triplet state to be redistributed among different vibrational levels. In perhaps the most promising data set presented in Figure 7(d), very little molecular population is detected in a spectroscopic position different than the initial one.

Among the possible reasons considered to understand these disappointing experimental results were: molecular ionisation, fine and hyperfine structure effects, parasitic coupling to electronic states different to the $(2)^3\Pi_g$ state and, in general, losses due to spontaneous emission to states not connected with the triplet ground state. A work in progress [54] shows that the chosen system cannot be considered 'closed' since the possibility of spontaneous emission from the $(2)^3\Pi_g$ to an electronic state other than the $a^3\Sigma_u^+$ ground triplet state is large (~25%). Thus, a large part of the population can be lost in each absorption–spontaneous emission cycle during the vibrational cooling process resulting in a failure of the vibrational cooling.

We can take into account these losses in our simulation. In Figure 8 we consider optical pumping of $a^3\Sigma_u^+$ triplet state molecules in the presence of losses equal to 25% per cycle. In (a) we use the simply shaped pulse considered also in Figure 7. As we see in the middle part of Figure 8(a), the particular shape of the Condon parabola is such, that this simply shaped pulse manages to excite transitions below the lower branch of the parabola (line of the first local maximum of the FC coefficients), as an optimised pulse would do [44]. Thus, the number of absorption–spontaneous emission cycles is minimised and the 39% of the

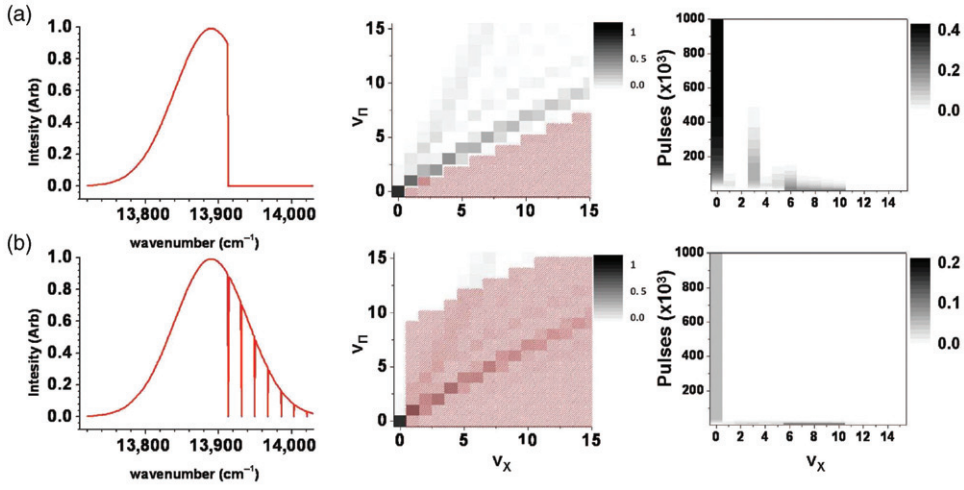

Figure 8. Simulation of the vibrational cooling of Cs_2 molecules in their $a^3\Sigma_u^+$ triplet state. In this simulation we consider an amount of 25% losses in each cooling cycle. In (a) are shown the results of the simulation of cooling with a simply shaped pulse. Due to the particular shape of the Condon parabola, the number of excitation–spontaneous emission cycles is minimised and 39% of the molecules are accumulated in the $v_X = 0$ vibrational level. In (b) a less favourable case, where only frequencies resonant to excitation of the $v_X = 0$ to any v_A level are removed. As a result, both branches of the Condon parabola are excited as shown in the middle. In the simulation on the right, we see that only 5% of the molecules are accumulated in the ground vibrational state.

molecules are accumulated in the $v_X = 0$ vibrational level. Such a result shows that a percentage of 25% of losses in each cycle does not justify the preliminary negative results shown in Figure 7(d). However, more losses could be present and not yet identified as spontaneous emission to different levels, pre-dissociation and more. Leaving this for a future work [54], we continue our theoretical study of the effect of the spontaneous emission losses, by considering a less favourable situation where this percentage of losses can be fatal for the optical pumping process. In part (b), we consider a pulse in which only the frequencies resonant to the transitions from $v_X = 0$ to any v_Π level are removed, and which is displayed on the left. Such a pulse excites both the branches of the Condon parabola, as we see in the middle. As a result, the number of required absorption–spontaneous emission cycles is raised, and almost all molecular population is lost, since only 5% is accumulated in the $v_X = 0$ vibrational level.

4. Application to rotational cooling

The use of optical pumping to cool molecular rotation has been discussed in some previous publications of our group [44,55,56]. An important aspect of the molecular cooling via optical pumping is the effect of the vibrational cooling laser field on the rotation and vice versa [56]. The cooling fields discussed in this article, treat the vibration and the rotation separately, i.e. when vibrational cooling is considered, the rotational degrees of freedom are omitted. As an example, in Figure 9(a) a simulation of the vibrational cooling in cesium dimers with the use of a simply shaped pulse is shown in the left part. In the middle, the modification induced on the vibrational distribution is shown, while in the right part we show the rotational distribution in the first three vibrational levels. In this simulation, we consider ten rotational levels in each vibrational state, while the molecular distribution is initially in the state with $J = 5$. The rotational distribution is spreading under the influence of the vibrational cooling field. The

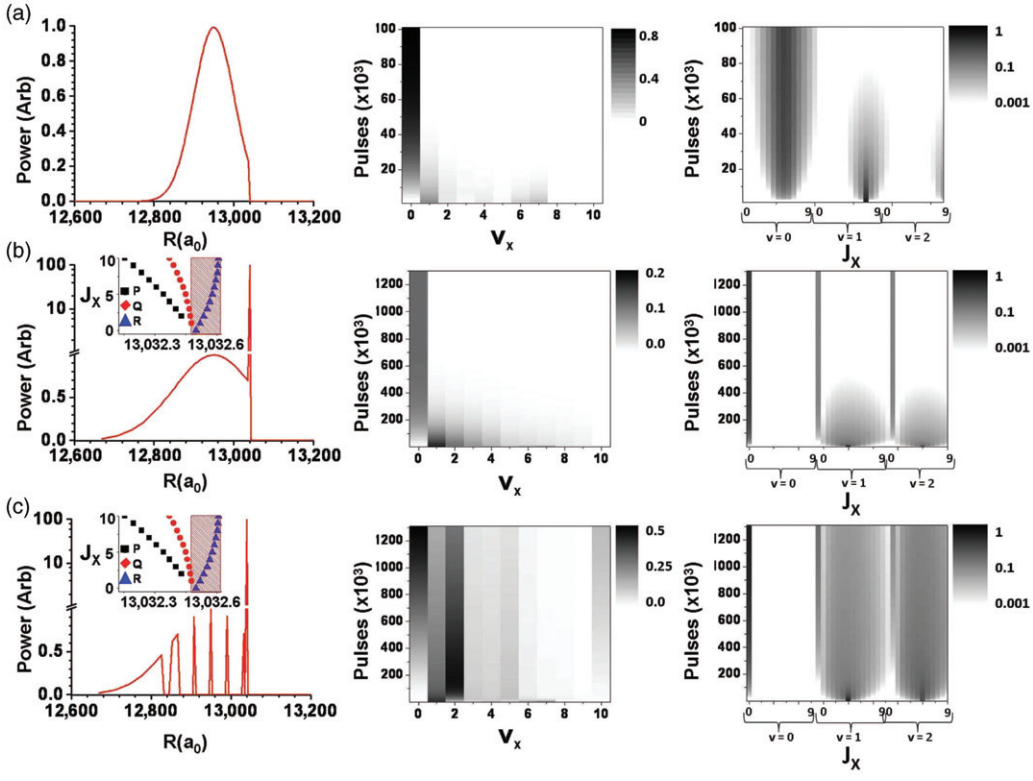

Figure 9. (a) A simulation of the vibrational cooling process with the use of a simply shaped pulse shown on the left. In the middle, we see the modification in the vibrational distribution and on the right the result on the rotational distribution. (b) Attempt to simultaneously cool the vibration and the rotation with a simply shaped pulse and an additional rotational cooling field (left). The high intensity peak is the field designed to cool rotation exciting only the P and Q branches (see inlet). The evolution of the vibrational distribution (middle) and the rotational distribution (right) shows that the simply shaped pulse cannot efficiently compensate for the vibrational heating effect. (c) The situation is improved if optimised pulses are considered for the vibrational cooling, and almost 50% of the molecular population is now accumulated in the absolute ground state.

only reason that this effect is not reflected on the experimental data, is that the pulsed REMPI detection is broadband enough in order to simultaneously probe all rotational levels. A similar optical pumping process designed to cool the molecular rotation would have a similar heating effect on the vibration. However, the molecular population would be spread over much larger energy and its simultaneous detection would be impossible. Thus, a field designed to cool the molecular rotation via optical pumping should be accompanied by a vibrational cooling field sufficient to cancel the vibrational heating effect.

A natural possibility for laser cooling of the molecular rotation is to consider a laser field shaped so that the frequencies corresponding to the transitions $\Delta J = J_e - J_X = 0, +1$ (Q and R bands) are removed (here J_e and J_X represent the rotational quantum numbers in the excited and ground levels respectively), and leave only the $\Delta J = J_e - J_X = -1$ (P band) ones that are J lowering (except the $J_X = 1 \rightarrow J_e = 1$ that is needed to empty the $J_X = 1$ level). With such a shaping, absorption–spontaneous emission cycles would indeed lead to a decrease on average of the principal rotation quantum number J_X, i.e. to laser cool the rotation. Unfortunately, it is not always possible for the P, Q and R branches to be resolved. In some cases, rotational cooling can be achieved on exciting both the P and Q bands. However, population transfer to the ground ro-vibrational level now requires more absorption–spontaneous emission steps than in the case where selective excitation of the P band alone is possible. This is the case when cooling molecular rotation via the same X electronic potential as for vibration is considered. In order for rotational cooling to be observed, the vibrational heating produced by the rotational cooling field must be compensated for and an efficient vibrational cooling process has to be used.

In Figure 9(b) we see that a simply shaped pulse is not enough to efficiently compensate the heating effect of the rotational cooling field. The fields in use are shown on the left. The peak shown out of scale on the right is 100 times more intense than the previous broadband pulses and it is identical to the one shown in Figure 9(a). The broadband part is the usual laser field that has been used for the vibrational cooling, as in part (a), but the bandwidth is doubled. Even with the increased bandwidth, the simply shaped pulse cannot efficiently compensate the vibrational heating. This is demonstrated both by the resulting vibrational distribution shown in the middle and by the rotational distribution shown on the right, since less than 20% of the molecular population is finally transferred to the ground ro-vibrational state. Conversely, if an optimised pulse of the same bandwidth is considered for the vibrational cooling, the situation is highly improved, as ~50% of the molecular population is accumulated in the ground ro-vibrational level, as shown in the simulation shown in Figure 9(c).

5. The case of the NaCs

We now consider the generalisation of the vibrational cooling technique to heteronuclear molecules. As stressed in Section 1, the interest in polar heteronuclear molecules is very large, since they are promising candidates for a variety of exotic applications.

The first step towards the realisation of an optical pumping process is to choose the transition through which the optical pumping process and the vibrational cooling will take place. As explained for the case of Cs_2 molecules, the feasibility of the cooling process depends on the shape of the Condon parabola, which if favourable, allows population transfer towards lower vibrational levels.

However, the choice for the excited state used for the optical pumping process has to be done according to an additional criterion, which is the minimisation of the losses towards different electronic states due to spontaneous emission. In other words, the chosen transition should be suitable for vibrational cooling (small equilibrium distance separation thus favourable for the Condon parabola) and at the same time as 'closed' as possible. Rigorous consideration of the various spontaneous emission losses during the vibrational cooling process, can be more complicated for heteronuclear molecules in comparison to the homonuclear ones, since the breakdown of the $g \rightarrow u$ symmetry increases the possible loss channels. For instance in the heteronuclear case, due to its spin–orbit coupling with the $b^3\Pi$ state, the use of the $A^1\Sigma^+$ state as an intermediate level for the optical pumping of the $X^1\Sigma^+$ would lead to losses toward the $a^3\Sigma^+$ state. Note that in the homonuclear case, the $A^1\Sigma_u^+$ state would only decay toward the $X^1\Sigma_g^+$ despite coupling with the $b^3\Pi_u$ state.

The molecule we have considered as an example for heteronuclear alkalis is NaCs, which has already been prepared in low ro-vibrational states and electrostatically trapped [57,58]. We based our study on molecular potentials and transition dipole moments provided by theoreticians in our laboratory [59]. Figure 10(a) shows the potential energy curves of the NaCs molecule. For this first fast study we choose to study transitions between the ground $(1)^1\Sigma$ and the $^1\Pi$ states, in order to avoid any discussion concerning the loss created if using the complex $A - b$. Here, the relatively strong variation of the transition dipole moment upon the

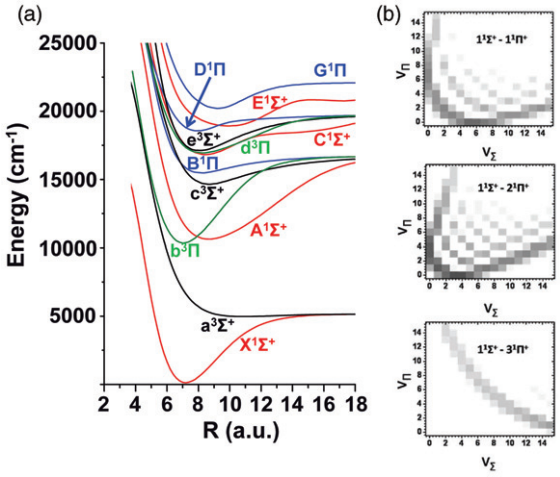

Figure 10. (a) Potential energy curves (PECs) of NaCs. (b) The Condon parabolas corresponding to transitions between the X(1)$^1\Sigma$ and the first three $^1\Pi$ states.

internuclear separation forces us to include it in the calculation for the Franck–Condon coefficients, to provide generalised FC coefficients, which are no longer summed to one and do not correspond to probability. Nevertheless, the parabolas generated by plotting these generalised coefficients, and which are displayed in Figure 10(b) for the first three $^1\Pi$ states, provide more accurate tools that can be used to design the vibrational cooling field in a similar way as the ordinary Condon parabolas.

As shown in Figure 10(b), the Condon parabolas corresponding to transitions between the X$^1\Sigma$ and the first three $^1\Pi$ states in NaCs are very different to the ones corresponding to the transitions of the Cs_2 molecule we have discussed earlier. The parabolas are touching the v_X axis in an excited vibrational level and thus the value of the FC coefficients for the first vibrational levels is relatively small. The exact point at which the parabola touches the v_X axis depends on the equilibrium distance separation between the electronic potentials involved in the transition. The difference between the equilibrium distances between ground and excited molecules is minimum for transitions between the $X^1\Sigma$ and the (2)$^1\Pi$ state. As far as the dynamics displayed by Condon parabolas are concerned, this is the best choice as a transition for the vibrational cooling process.

Let us examine initially the choice of the D(2)$^1\Pi$ as an excited state for the optical pumping process, since it leads to the most favourable Condon parabola. The losses are estimated in this case to be ~7% per optical pumping cycle, i.e. we consider this percentage of the excited molecular population lost during the spontaneous emission process. The estimation of the losses towards a different electronic potential is done in a very crude way, assuming constant and identical dipole moment for all transitions, i.e. by calculating the ratio $(E_e - E_g)^3/(E_e - E_l)^3$, where with E_e and with E_g we note the energy of the excited and the ground state of the optical pumping, while with E_l we note the energy of the electronic state to which the lost population is transferred.

Figure 11(a) shows the results of a simulation of vibrational cooling in NaCs, with the D(2)$^1\Pi$ state as the excited state of the optical pumping process. The pulses have a Gaussian shape, five times bigger bandwidth and similar intensity to the ones considered for the case of cesium dimers. Vibrational population is initially distributed equally in the vibrational levels with $v_X = 1$–10 levels. In the upper part we show the shaping considered for the femtosecond pulses. The addressed transitions are noted with red hatched squares on top of the Condon parabola shown in the middle. The general idea is to create a pulse which excites the lower part of the Condon parabola, as if we intend molecular population transfer to the $v_X = 3$ level where the 'Condon' parabola hits the v_X axis. Population transfer towards this level is favoured by the shape of the Condon parabola and it could be achieved simply by exciting its lower part and keeping this level dark. Here however, our goal is population transfer to the $v_X = 0$ ground vibrational level, thus we keep the $v_X = 0$ level dark, while population is 'stolen' from the $v_X = 3$ level by addressing the $v_X = 3 \Rightarrow v_A = 0$, 3 transitions. Such a pulse can result in the transfer of ~65% of the total molecular population to the $v_X = 0$ state, in the presence of losses estimated to be ~7%.

Finally, in Figure 11(b), we examine the choice of the B(1)$^1\Pi$ as the excited state of the optical pumping process. This choice minimises losses due to spontaneous emission on the one hand, but on the other it leads to a less favourable Condon parabola, similar to the one displayed in Figure 6(b). As previously explained, consideration of a molecular population transfer to the $v_X = 0$ ground vibrational level would require a bandwidth almost three times larger. Furthermore, optical pumping would spread the molecular population to more vibrational levels and the number of the absorption–spontaneous emission cycles required for the cooling would be bigger, increasing the effect of the losses due to spontaneous emission on the cooling process efficiency.

However, there are interesting processes which can be successfully realised without considering more broadband fields. As an example, we consider as goal for the process not to transfer population to the $v_X = 0$ ground vibrational level but to transfer the molecular population to the $v_X = 6$ state, which is favoured by the

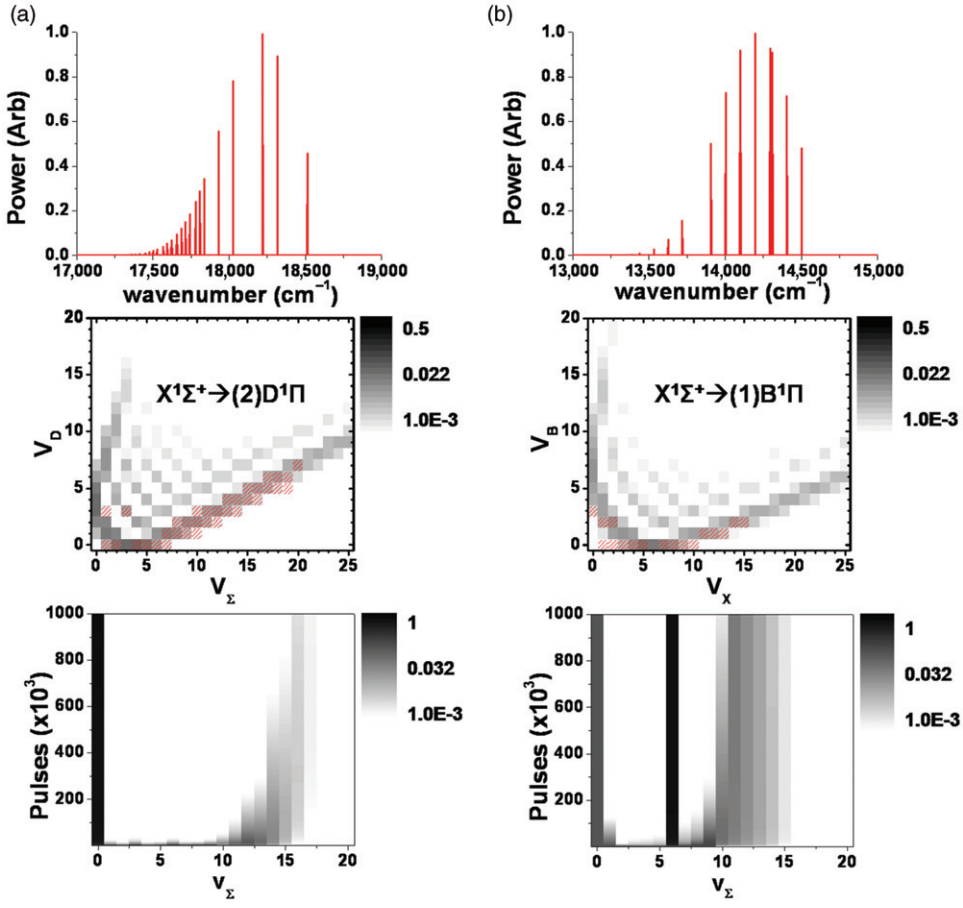

Figure 11. (a) Simulation of vibrational cooling in NaCs: optical pumping is considered between the $^1\Sigma^+$ and the $(2)^1\Pi$ state. In the upper part we show the femtosecond pulse. The addressed transitions are noted with red hatched squares on top of the Condon parabola shown in the middle. In the lower part we see the result of the simulation showing that $\sim 65\%$ of the molecular population is transferred to the $v_X = 0$ ground vibrational level. Losses due to spontaneous emission equal to 7% per optical pumping cycle, are taken into account in this simulation. (b) Simulation of molecular population transfer to the $v_X = 6$ level in NaCs. Now, the optical pumping process is considered between the $X^1\Sigma^+$ and the $(1)^1\Pi$ state, a choice which reduces the losses due to spontaneous emission to 4% per optical pumping cycle. The pulse shown in the upper part addresses transitions situated in the lower part of the Condon parabola as shown in the middle, and achieves transfer of $\sim$71% to the target level.

Condon parabola. In the upper part of Figure 11(b), we show the considered shaping while in the middle we show the addressed transitions on the corresponding Condon parabola. The result of the simulation shown in the lower part, is that $\sim$71% of the molecular population is transferred in the target state $v_X = 6$ in the presence of losses estimated to be $\sim$ 4% in each optical pumping cycle.

6. Conclusions

We have studied experimentally how femtosecond pulse shaping techniques can be used to realise efficient vibrational cooling by optical pumping of cold Cs_2 molecules. The method demonstrated here is based on a light source spectrally broad enough to excite all populated vibrational levels and shaped in amplitude in order to eliminate all frequencies that could excite the desired target $v_X = 0$ level.

We have also demonstrated the optical pumping to single vibrational levels such as $v_X = 0, 1$ with two different shaping methods. The simple shaping method enjoys experimental and conceptual simplicity. However, the limited efficiency of this simple shaping method does not allow one to consider several important applications, such as cooling Cs_2 molecules in their triplet states, cooling the rotation, cooling the vibration in heteronuclear molecules and in particular in NaCs, and direct laser cooling of molecules.

These interesting generalisations of the initial experiments [29,44] can be considered with the use of

the new, more sophisticated shaping method discussed here. The method takes into consideration the details of the Condon parabola that govern the dynamics of the optical pumping process, and provides vibrational cooling schemes of increased efficiency, both for the number of molecules transferred in the desired state and for the number of absorption–spontaneous emission cycles required. Such an advanced pulse shaping method might allow important breakthroughs in the field of cold molecules. The current efficiency of the optical pumping is mainly limited by the finite laser spectral bandwidth and the imperfect extinction ratio of our LC-SLM. In principle, the theory indicates that the use of broader sources and better extinction ratio would allow up to 100% transfer of population in one single vibrational level, hopefully opening the way to direct laser cooled molecules.

A further step in this direction has been accomplished. In fact, we have recently demonstrated that optical pumping in molecules can be realised also with an incoherent light source [60]. This means that a wide variety of sources, including LEDs, can be used for molecular cooling, as long as it is possible to perform amplitude shaping. This reduces a lot the complexity and cost of the experimental apparatus required for the realisation of optical pumping in molecules and permits the consideration of even more complicated processes.

Acknowledgements

This work is supported in Orsay by the 'Institut Francilien de Recherche sur les Atomes Froids' (IFRAF). In Toulouse, it is supported by the Agence Nationale de la Recherche (Contract ANR – 06-BLAN-0004) and the Del Duca foundation. M.P. acknowledges sabbatical support at the Laboratoire Aimé Cotton from Goucher College. A.F. and M.P. have been supported by the 'Triangle de la Physique' under contracts 2007-n.74T and 2009-035T 'GULFSTREAM' and 2008-n.07T 'QCCM' (Quantum Control of Cold Molecules). M.A. thanks the EC-Network EMALI, the 'Université Franco-Italienne' (Galileo Project) and the partnership between the Université Paris Sud and the University of Pisa (COGITO). We thank Nadia Bouloufa and Olivier Dulieu for providing us with the FC calculations.

Note
All figures can be viewed in colour online.

References

[1] H. Rabitz, R. de Vivie-Riedle, M. Motzkus and K. Kompa, Science **288**, 824 (2000).
[2] M. Shapiro and P. Brumer, *Principles of the Quantum Control of Molecular Processes* (Wiley-Interscience, Hoboken, NJ, 2003).
[3] D. D'Alessandro, *Introduction to Quantum Control and Dynamics* (Chapman and Hall, Boca Raton, 2007).
[4] R.V. Krems, Phys. Chem. Chem. Phys. (incorporating Faraday Trans.) **10**, 4079 (2008).
[5] I.W.M. Smith, *Low Temperatures and Cold Molecules* (Imperial College Press, London, 2008).
[6] K. Roman, F. Bretislav and C. William, *Cold Molecules: Theory, Experiment, Applications* (Taylor & Francis, Abingdon, 2009).
[7] O. Dulieu and C. Gabbanini, Rep. Progr. Phys. **72**, 086401 (2009).
[8] M.T. Bell and T.P. Softley, Mol. Phys. **107** (2), 99 (2009).
[9] H. Metcalf and P. van der Straten, *Laser Cooling and Trapping* (Springer, Berlin, 1999).
[10] J.T. Bahns, W.C. Stwalley and P.L. Gould, J. Chem. Phys. **104**, 9689 (1996).
[11] S.Y.T. van de Meerakker, H.L. Bethlem and G. Meijer, Nature Phys. **4**, 595 (2008).
[12] T. Köhler, K. Góral and P.S. Julienne, Rev. Mod. Phys. **78**, 1311 (2006).
[13] C. Chin, R. Grimm, P. Julienne and E. Tiesinga, preprint, ArXiv 0812.1496 (2008). http://adsabs.harvard.edu/abs/2008arXiv0812.1496C
[14] K.M. Jones, E. Tiesinga, P.D. Lett and P.S. Julienne, Rev. Mod. Phys. **78**, 483 (2006).
[15] F. Lang, K. Winkler, C. Strauss, R. Grimm and J.H. Denschlag, Phys. Rev. Lett. **101** (13), 133005 (2008).
[16] J.G. Danzl, M.J. Mark, E. Haller, M. Gustavsson, R. Hart, A. Liem, H. Zellmer and H.-C. Nägerl, New J. Phys. **11** (5), 055036 (2009).
[17] K. Ni, S. Ospelkaus, M.H.G. de Miranda, A. Péer, B. Neyenhuis, J.J. Zirbel, S. Kotochigova, P.S. Julienne, D.S. Jin and J. Ye, Science **322**, 231 (2008).
[18] K. Ni, S. Ospelkaus, D.J. Nesbitt, J. Ye and D.S. Jin, Phys. Chem. Chem. Phys. (incorporating Faraday Trans.) **11**, 9626 (2009).
[19] A.N. Nikolov, E.E. Eyler, X.T. Wang, J. Li, H. Wang, W.C. Stwalley and P.L. Gould, Phys. Rev. Lett. **82**, 703 (1999).
[20] J.M. Sage, S. Sainis, T. Bergeman and D. Demille, Phys. Rev. Lett. **94** (20), 203001 (2005).
[21] J. Deiglmayr, A. Grochola, M. Repp, K. Mörtlbauer, C. Glück, J. Lange, O. Dulieu, R. Wester and M. Weidemüller, Phys. Rev. Lett. **101** (13), 133004 (2008).
[22] B.L. Brown and I.A. Walmsley, J. Phys. B At. Mol. Phys. **39**, 1055 (2006).
[23] C.P. Koch and R. Moszyński, Phys. Rev. A **78** (4), 043417 (2008).
[24] E. Kuznetsova, M. Gacesa, P. Pellegrini, S.F. Yelin and R. Côté, New J. Phys. **11** (5), 055028 (2009).
[25] S. Kallush and R. Kosloff, Phys. Rev. A **77** (2), 023421 (2008).
[26] C.P. Koch, Phys. Rev. A **78** (6), 063411 (2008).
[27] P. Marquetand and V. Engel, J. Phys. B At. Mol. Phys. **41** (7), 074026 (2008).

[28] S. Ghosal, R.J. Doyle, C.P. Koch and J.M. Hutson, New J. Phys. **11** (5), 055011 (2009).
[29] M. Viteau, A. Chotia, M. Allegrini, N. Bouloufa, O. Dulieu, D. Comparat and P. Pillet, Science **321**, 232 (2008).
[30] C. Brif, R. Chakrabarti and H. Rabitz, preprint, ArXiv 0912.5121 (2009). http://adsabs.harvard.edu/abs/2009arXiv0912.5121B
[31] A. Bartana, R. Kosloff and D.J. Tannor, J. Chem. Phys **99**, 196 (1993).
[32] D.J. Tannor, R. Kosloff and A. Bartana, Faraday Discuss. **113**, 365 (1999).
[33] S.G. Schirmer, Phys. Rev. A **63** (1), 013407 (2000).
[34] A. Bartana, R. Kosloff and D.J. Tannor, Chem. Phys. **267**, 195 (2001).
[35] W. Salzmann, U. Poschinger, R. Wester, M. Weidemüller, A. Merli, S.M. Weber, F. Sauer, M. Plewicki, F. Weise, A.M. Esparza, L. Wöste and A. Lindinger, Phys. Rev. A **73** (2), 023414 (2006).
[36] B.L. Brown, A.J. Dicks and I.A. Walmsley, Phys. Rev. Lett. **96** (17), 173002 (2006).
[37] A.M. Weiner, Rev. Sci. Instrum. **71** (5), 1929 (2000).
[38] A. Assion, T. Baumert, M. Bergt, T. Brixner, B. Kiefer, V. Seyfried, M. Strehle and G. Gerber, Science **282**, 919 (1998).
[39] A. Monmayrant, B. Chatel and B. Girard, Phys. Rev. Lett. **96** (10), 103002 [<http://link.aps.org/abstract/PRL/v96/e103002>] (2006).
[40] J.L. Herek, W. Wohlleben, R.J. Cogdell, D. Zeidler and M. Motzkus, Nature **417** (6888), 533 (2002).
[41] A. Efimov, M.D. Moores, B. Mei, J.L. Krause, C.W. Siders and D.H. Reitze, Appl. Phys. B **70**, S133 (2000).
[42] H.P. Sardesai, C.C. Chang and A.M. Weiner, J. Lightwave Technol. **16** (11), 1953 (1998).
[43] A. Monmayrant and B. Chatel, Rev. Sci. Instrum. **75**, 2668 (2004).
[44] D. Sofikitis, S. Weber, A. Fioretti, R. Horchani, M. Allegrini, B. Chatel, D. Comparat and P. Pillet, New J. Phys. **11**, 055037 (2009).
[45] M. Viteau, A. Chotia, M. Allegrini, N. Bouloufa, O. Dulieu, D. Comparat and P. Pillet, Phys. Rev. A (At. Mol. Opt. Phys.) **79** (2), 021402 (2009).
[46] M. Raab, G. Höning, W. Demtröder and C.R. Vidal, J. Chem. Phys. **76**, 4370 (1982).
[47] M.M. Wefers and K.A. Nelson, J. Opt. Soc. Am. B **12** (7), 1343 (1995).
[48] G. Stobrawa, M. Hacker, T. Feurer, D. Zeidler, M. Motzkus and F. Reichel, Appl. Phys. B **72** (5), 627 (2001).
[49] O.E. Martinez, IEEE J. Quantum Electron. **QE-23** (1), 59 (1987).
[50] W. Weickenmeier, U. Diemer, M. Wahl, M. Raab, W. Demtröder and W. Müller, J. Chem. Phys. **82**, 5354 (1985).
[51] U. Diemer, R. Duchowicz, M. Ertel, E. Mehdizadeh and W. Demtröder, Chem. Phys. Lett. **164**, 419 (1989).
[52] A. Chotia, M. Viteau, T. Vogt, D. Comparat and P. Pillet, New J. Phys. **10** (4), 045031 (2008).
[53] N. Bouloufa, E. Favilla, M. Viteau, A. Chotia, A. Fioretti, C. Gabbanini, M. Allegrini, D. Comparat, O. Dulieu and P. Pillet, Mol. Phys. in preparation (2010).
[54] N. Bouloufa, M. Pichler and O. Dulieu, private communication (2009).
[55] D. Sofikitis, A. Fioretti, S. Weber, M. Viteau, A. Chotia, R. Horchani, M. Allegrini, B. Chatel, D. Comparat and P. Pillet, Chin. J. Chem. Phys. **22** (2), 149 [<http://stacks.iop.org/1674-0068/22/149>] (2009).
[56] A. Fioretti, D. Sofikitis, R. Horchani, X. Li, M. Pichler, S. Weber, M. Allegrini, B. Chatel, D. Comparat and P. Pillet, J. Mod. Opt. **78**, 2089 (2009).
[57] C. Haimberger, J. Kleinert, P. Zabawa, A. Wakim and N.P. Bigelow, New J. Phys. **11** (5), 055042 (9pp) [<http://stacks.iop.org/1367-2630/11/055042>] (2009).
[58] J. Kleinert, C. Haimberger, P.J. Zabawa and N.P. Bigelow, Rev. Sci. Instrum. **78**, 113108 (2007).
[59] M. Aymar and O. Dulieu, Mol. Phys. **105**, 11 (2007).
[60] D. Sofikitis, R. Horchani, X. Li, M. Pichler, M. Allegrini, A. Fioretti, D. Comparat and P. Pillet, Phys. Rev. A **80** (5), 051401 (2009).